Journal of Alloys and Compounds 661 (2016) 476–482

Contents lists available at ScienceDirect

Journal of Alloys and Compounds

journal homepage: http://www.elsevier.com/locate/jalcom

Microstructure evolution of V–Al–C coatings synthesized from a V_2AlC compound target after vacuum annealing treatment

Zhenyu Wang [a], Xiaowei Li [a], Jie Zhou [b], Pei Liu [a], Qing Huang [b], Peiling Ke [a, *], Aiying Wang [a, **]

[a] Key Laboratory of Marine Materials and Related Technologies, Zhejiang Key Laboratory of Marine Materials and Protective Technologies, Ningbo Institute of Materials Technology and Engineering, Chinese Academy of Sciences, Ningbo, 315201, China
[b] Functional Materials Division, Ningbo Institute of Materials Technology and Engineering, Chinese Academy of Sciences, Ningbo, 315201, China

ARTICLE INFO

Article history:
Received 14 September 2015
Received in revised form
6 November 2015
Accepted 23 November 2015
Available online 26 November 2015

Keywords:
V_2AlC coating
Magnetron sputtering
Microstructure
Mechanical properties
Tribological behavior

ABSTRACT

V_2AlC belongs to a family of ternary nano-laminate alloys known as the MAX phases, which exhibit a unique combination of metallic and ceramic properties. In this work V–Al–C coatings with deposited $(V,Al)_2C$ nano-crystallines and amorphous phase were magnetron sputtered from V_2AlC compound target. The subsequent vacuum annealing for 1 h was carried out at 600 °C, 700 °C and 800 °C, respectively. The crystallization of V_2AlC MAX phase was detected by annealing at 600 °C. Meanwhile, a small amount of amorphous carbon phase appeared. Further increasing annealing temperature to 700 °C led to a complete transformation from amorphous V–Al–C phase to V_2AlC phase, as well as a significant increase in the amorphous carbon content. It was noticed that the crystallinity of V_2AlC phase was significantly enhanced and amorphous carbon was almost disappeared after annealing at 800 °C. The coating toughness became better with the increase in the content of V_2AlC MAX phase. The optimized mechanical and tribological properties of the annealed V–Al–C coatings were further discussed in terms of the microstructure evolution.

1. Introduction

V_2AlC (space group $P6_3/mmc$) belongs to a family of the so-called $M_{n+1}AX_n$ phases, where M is a transition metal, A is an A group element, X is either C or N, and n = 1–3. A distinctive feature of these phases is their layered structure with alternating $M_{n+1}X_n$ and A layer, the carbon atoms occupying the octahedral voids formed by M atoms, without contact with atoms A. MAX phases are well known for their high stiffness, good mechanical stability as well as chemical and thermal resistance, which are typical properties of ceramic materials. At the same time, they exhibit good electrical and thermal conductivity, as well as facile machinability, almost in the range of metallic materials [1]. Due to their unique structure and interesting performances, MAX phases have been fabricated in form of both bulk materials [2] and in coatings [3].

Compared to the bulk forms, recently, MAX phase coating synthesized by physical vapor deposition (PVD), in particular, have drawn much attentions due to its promising feasibility in the used substrates and deposited large area for wide range of applications. Variety of MAX coatings including Ti_2AlC, Cr_2AlC, Ti_2AlN and Ti_3SiC_2, have been achieved by PVD techniques, where the deposition process, mechanical properties and oxidation resistance of coatings are investigated systematically. Nevertheless, few studies about the V-containing 211 phase V_2AlC coating are reported. V-based coatings exhibit lower friction coefficient compared to that of Ti or Cr-based coatings [4], V_2AlC MAX phase coatings is considered as a strong candidate for supertough wear-resistant application. Until now, the V_2AlC coatings have been synthesized using magnetron sputtering techniques either from elemental targets or from compound targets at relatively high substrate temperature or alternated by the post annealing. Growth of V_2AlC coatings was reported in 2006 by Schneider et al. [5] utilizing sputtering from three elemental targets at 850 °C substrate temperature. Sigumonroung et al. [6] believed that the threshold temperature range for the formation of phase pure V_2AlC using vapor condensation without ion assistance lied between 650 and 750 °C. Jiang et al. [7] studied the effects of post-annealing temperature (550–850 °C) on the thermal stability and the phases formation of the vanadium

* Corresponding author.
** Corresponding author.
E-mail addresses: kepl@nimte.ac.cn (P. Ke), aywang@nimte.ac.cn (A. Wang).

http://dx.doi.org/10.1016/j.jallcom.2015.11.170
0925-8388/

carbide solid solution $(V,Al)_2C_x$ coatings. They found that the formation of V_2AlC MAX phase could be observed at 650 °C and phase-pure V_2AlC emerged at 850 °C. The crystallization kinetics of the deposited X-ray amorphous V_2AlC coatings was investigated by Abdulkadhim et al. [8], where the crystalline V_2AlC phase formed between 565 and 675 °C. Obviously, the structure of V–Al–C coating phase are significantly dependent upon the deposition and annealing temperature, it is crucial to clarify the correlation between the microstructure evolution and physichemcial properties of coating during the formation for its expected applications.

Moreover, the advantages of Ti alloys over other metallic materials lie in their good combination of mechanical and chemical properties, such as high stiffness, low density, good corrosion resistance. Ti-6Al-4V (TC4) is being a family member of titanium alloy, which is one of the most promising alternative lightweight heat resistant alloys. In addition, TC4 can be easily welded, forged and machined [9,10], which makes it more wide applications. Here, the V–Al–C coatings were deposited on TC4 substrate by DC magnetron sputtering using a powder sintered composite target with a pure V_2AlC phase in an industrial deposition chamber, which was followed by a thermal annealing in vacuum from 600 to 800 °C. The aim of this work is to examine the role of deposition and post-annealing process on the structure, mechanical and tribological properties of V–Al–C coating. The results showed that the higher content of the formed V_2AlC MAX phase, the better toughness of coating was. The special layered structure of MAX phase emerged in the coating after thermal annealing was considered as the key role for the controllable mechanical and tribological properties.

2. Experimental

V–Al–C coatings were deposited by a hybrid ion beam deposition system [11] consisting of a circular DC magnetron sputtering and a linear anode-layer ion sources (LIS). The samples of TC4 alloy with the size of 15 mm × 10 mm × 2 mm were chosen as the substrate in the present work. The nominal composition (wt.%) of the alloy is given as follows: Ti, bal; Al, 6; V, 4; Fe, 0.25; O, 0.15; C, 0.1; N, 0.04; H, 0.015. After being polished to 3000-grit, the substrates were ultrasonically cleaned in acetone and ethanol each for 15 min followed by a dried process in warm air. Then, the substrates were fixed on a rotary sample holder at a distance of 15 cm to the target. The base pressure was pumped less than 3×10^{-3} Pa. Prior to deposition, the substrates were sputter-cleaned for 15 min using Ar ions generated by LIS to remove the contaminants of surface. The magnetron cathode with a diameter of 80 mm was fulfilled by a compound target composing the single-phase V_2AlC, which was homemade by spark plasma sintering of elemental V, Al, and C powders with a molar ratio of 2:1.2:0.9 at 1500 °C for 30 min. The applied power density of sputtering target was 14 W/cm^2. During deposition the argon pressure was maintained at 0.77 Pa. The negative bias voltage of −150 V, with a frequency and duration of 350 kHz and 1.1 ms, was applied to the substrates without other intentionally heated. After 8 h deposition, the thickness of the coating was about 4 μm. Then, annealing treatment of the as-deposited coating was conducted at 600 °C, 700 °C and 800 °C in vacuum for 1 h. Before the annealing process, the chamber was pump down to 1.0×10^{-2} Pa and heated to the annealing temperature with a heating rate of about 4 °C/min.

The microstructures of the coating were investigated by the combined x-ray diffraction (XRD), scanning electron microscopy (SEM), and transmission electron microscopy (TEM). Structural analysis was carried out using x-ray diffraction (XRD), with a BrukerD8 Advance diffractometer, using Cu Kα radiation. The detected phase content was calculated on the basis of XRD pattern refinement [12]. The surface secondary electrons morphology was examined by a Hitachi S4800 high resolution SEM. The cross-section backscattered electrons morphology was examined by a FEI Quanta FEG 250 SEM, equipped with an energy-dispersive X-ray spectrometry (EDX) using an EDAX Sapphire Si (Li) detector. Quantification was performed using the standard ZAF method, which incorporated individual corrections from the atomic number (Z), absorption (A), and fluorescence (F). Cross-sectional TEM (XTEM) studies were performed on a JEOL 2100-HR system. Raman spectroscopy (InVia-reflex, Renishaw) equipped with a 60 mW He–Ne laser of 532 nm exciting wavelength was used to evaluate the carbon atomic bond structure in the coatings. Mechanical properties were measured by a MTS Nanoindenter G200 tool in a continuous stiffness measurement mode using a Berkovich diamond tip. Hardness and Young's modulus were determined using the Oliver-Pharr analysis [13]. The characteristic hardness was chosen in a depth of around 1/10 of the coating thickness, where the measured value was not affected by the substrate. Six replicate indentations were done for each sample.

Tribological behavior was evaluated by reciprocating ball-on-plate dry sliding tests against Al_2O_3 balls with a diameter of 6 mm on a UMT-3 tribometer (CETR, USA). The sliding speed and frequency were set at 0.01 m/s and 1 Hz, respectively. All tests were conducted under a load of 10 N at the ambient temperature (~293 K) and a relative humidity of 50–60%. The total sliding time was 3600 s. After tests, the wear track profiles were measured by the surface profilometer. The wear rates were evaluated as volume per sliding distance per load [14].

3. Results and discussion

Fig. 1 shows the XRD patterns of the pristine V–Al–C coatings and the annealed ones at 600 °C, 700 °C and 800 °C. A broad diffraction peak appeared at about 43° for the pristine coatings and no obvious crystalline peaks can be found within the XRD resolution limits, indicating that the pristine V–Al–C coatings were amorphous or some small nano-crystalline. This result was consistent with that obtained by Li [15] and Abdulkadhim et al. [8], where the amorphous Cr–Al–C and V–Al–C coatings were reported by sputtering the Cr_2AlC and V_2AlC composite target at the room temperature, respectively. A further careful examination was conducted by HRTEM in this study later. However, if one considers the MAX phases belong to the high-order material systems, in

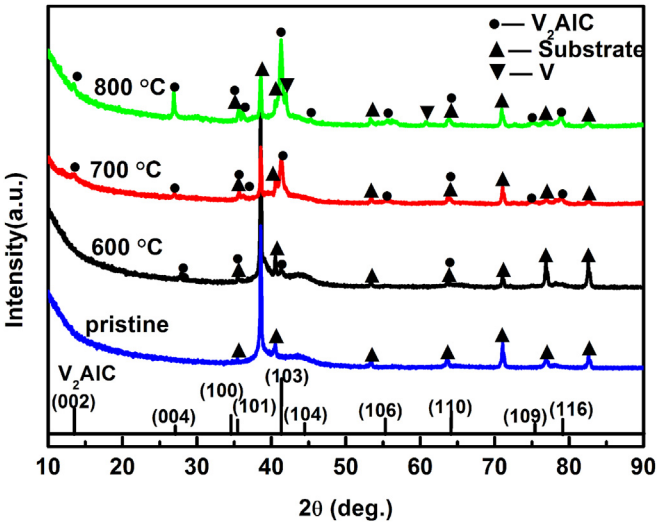

Fig. 1. XRD patterns of the pristine and annealed V–Al–C coatings at 600 °C, 700 °C and 800 °C.

which a significant amount of thermally activated atom diffusion is required to form these large-unit-cell phases, a high purity of MAX phase coatings could only be found in case of high deposition temperature or by post-annealing. As expected, it was particularly important that different with the pristine coating, the V_2AlC MAX phase had been evolved after the subsequent thermal annealing in range of 600–800 °C. When annealed in 600 °C for 1 h, a small amount of V_2AlC MAX phase (26.2 wt%) was detected. With increase of temperature to 700 °C, the diffraction intensity of V_2AlC phase increased and the V_2AlC phase content increased to about 98.16 wt%. The 2θ peak approximately at 13° identified the strengthened direction of (002) for the formed V_2AlC MAX phase. This diffraction signal is not prone to overlap with diffraction lines of other phases. Further increasing the annealed temperature to 800 °C, the crystallinity of V_2AlC MAX phase was enhanced and the preferential orientation was evolved into V_2AlC (103), where the V_2AlC phase content was estimated at around 98.09 wt%. In addition, a small peak at about 42° and 60.5° was likely to be attributed to the V impurity. This is due to the decomposition of part of V_2AlC phase at 800 °C, where the Al desorption occurs as a result of the weak bonding between Al and V atoms with a high activity under a high vacuum condition.

Raman spectroscopy is a non-destructive and fast method to characterize the hybridized bond for carbon materials. In order to further classify the atomic bond of carbon atoms in the V–Al–C coating, we performed the Raman test for the pristine and annealed coatings. As shown in Fig. 2, no obvious typical peak was found for the amorphous carbon feature. After annealing at 600 °C, the common feature of so-called D and G peaks in carbon materials, which lied at around 1360 cm^{-1} caused by the zone edge of A_{1g} breathing mode and 1600 cm^{-1} arising from E_{2g} symmetry stretching vibration mode [16], were visible in the spectra, indicating the amorphous carbon phase appeared in the coating. Noted that increasing the annealing temperature to 700 °C, the increased intensity of D and G peaks revealed the increase of amorphous carbon phases. However, this amorphous carbon feature disappeared dramatically in the spectra as the annealing temperature increased to 800 °C.

Fig. 3 shows the SEM surface morphologies of the pristine and the annealed coatings. As can be seen, both the particle size and shape differed significantly across the surface of the pristine and the annealed V–Al–C coatings. It was of particular that the pristine coating illustrated the cauliflower shape with the feature of amorphous phase. Increasing the annealing temperature from 600 °C to 700 °C enhanced the crystallinity of coatings. The minor grains as large as 50–150 nm covered the coating surface annealed at 600 °C, while it transferred to the rod- and cone-shaped grain morphology for the coating annealed at 700 °C. Moreover, the grain faces showed a clearly lamellar structure, indicating the typical feature for ternary layered carbides (MAX phases). When the coating was annealed at higher temperature at 800 °C, this lamellar structure with the grain interior nucleation became more distinct, which agreed well with the results of the Cr_2AlC and Ti_2AlC MAX phase coatings [17,18].

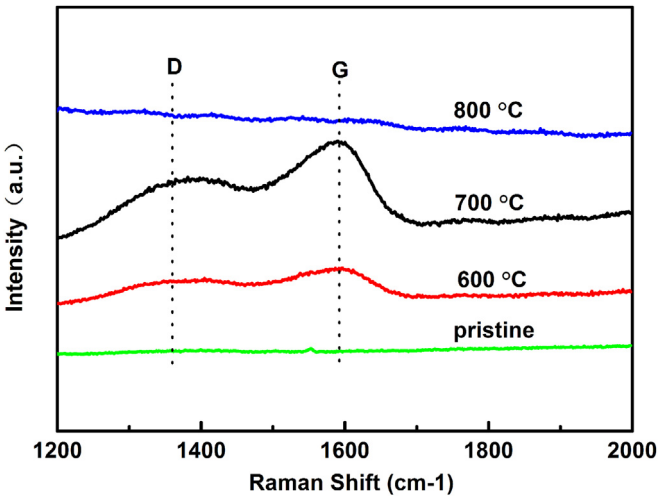

Fig. 2. Raman spectra of the pristine V–Al–C coatings and the annealed ones at 600 °C, 700 °C and 800 °C.

To further check the elemental diffusion during coating growth, Fig. 4 shows the cross-section of pristine coatings on the TC4 alloy substrate and annealed coatings at different temperature. It can be seen that no obvious difference appears between the pristine and annealed coatings, where all the coating thickness was approximately 4 μm and the coatings were uniform and crack-free. However, the interface between the coating and substrate was distinct after annealing, revealing no element diffusion occurred with limits of annealing below 800 °C. This result benefits us possibly to control the element composition content and obtain the high-purity MAX phase, foreseeing interesting potential applications. Furthermore, it can be postulated that the coating adhesion with MAX phases is good because of the observed tight bonding feature between the coatings and the substrate [19].

Fig. 5 shows the EDX measurement across line scan between the substrate and coating. For all samples, the composition sharply changed at the interface, demonstrating that no inter-diffusion occurred between the coating and the substrate within the limits of annealing temperature below 800 °C. Since, EDX could introduce large inaccuracy in the determination of light elements, C and O content calculation were not shown in the lines. The V/Al ratios of the coatings increased from 1.74 in pristine state to 2.13 as annealing temperatures was up to 800 °C monotonically. In fact, it is well-known that MAX phase materials possess a high element activity due to weak bonding between A and M atoms. Besides, metallic Al owns high vapor pressure beneath a high vacuum. As a consequence, when the temperature is beyond of 660 °C (the melting temperature of Al), the volatility of Al was enhanced, which led to the increase of V/Al ratios and decomposition of V_2AlC phase. As for the MAX phases, evaporative loss of the A element during coating growth has been observed in several MAX phase studies. Frodelius et al. [20] reported Al deficiency during deposition of Ti_2AlC MAX phase from a Ti_2AlC compound target. Deficiency of other A-elements also was found in the Ti–Si–C, V-Ge-C, and Cr–Al–C systems [21–23]. Interesting result is that in the present works, although V/Al atomic ratio deviated from the stoichiometric of V_2AlC phase, V_2AlC MAX phase can also be formed, indicating that MAX phase coatings can be formed in a suitable composition range. Mertens et al. [24] synthesized pure Cr_2AlC MAX phase coatings by the combinatorial DC magnetron sputtering at 800 °C with Cr/Al atomic ratio of 1.42–2.03, and V_2AlC MAX phase was observed to be formed at 850 °C with V/Al of 1.71–2.08 by Schneider [5], which were consistent well with our results.

According to the above discussion, we performed the HRTEM characterization to further reveal the microstructures of the pristine and the annealed coatings, in particular to determine whether the V_2AlC MAX phases were evolved in nanoscale or microscale feature after annealing. Fig. 6 shows the plan-view bright field TEM image for the pristine coating, together with the corresponding selected area electron diffraction (SAED) pattern inserted in Fig. 6a. It is distinct that the as-deposited coating is not exact amorphous as those reported in other literature [8,15], but $(V,Al)_2C$-nanocrystals (size less than 5 nm) were dispersed within the amorphous matrix.

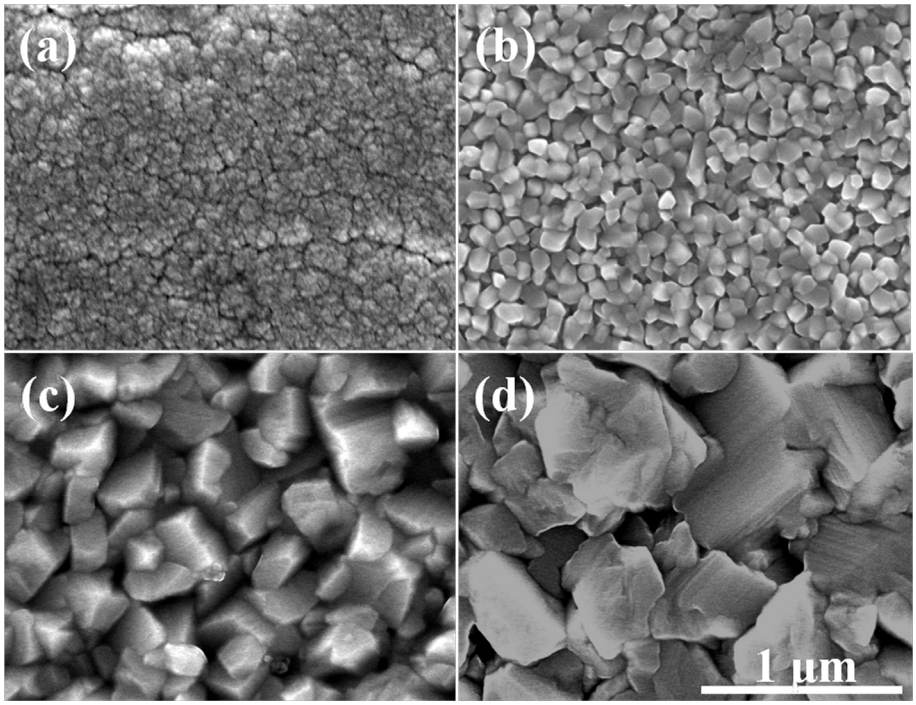

Fig. 3. Surface morphologies of the V–Al–C coatings: (a) pristine, (b) annealed at 600 °C, (c) 700 °C and (d) 800 °C.

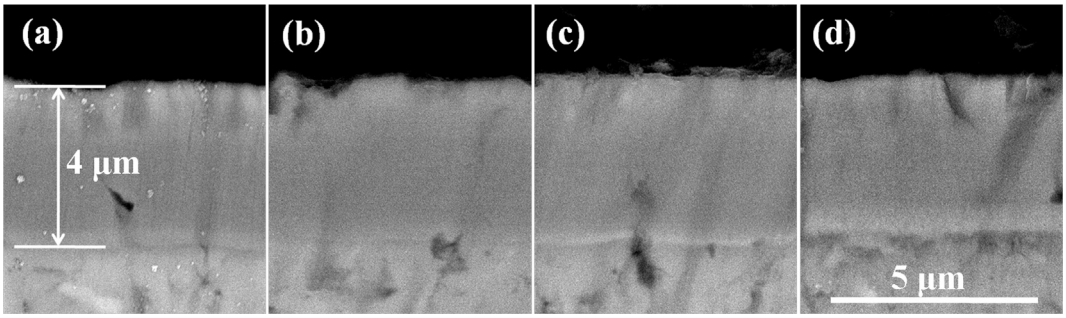

Fig. 4. Cross-section morphologies of the V–Al–C coatings: (a) pristine, (b) annealed at 600 °C, (c) 700 °C and (d) 800 °C.

In Fig. 6c, the lattice fringes could be attributed to (121) planes of the $(V, Al)_2C$ phase, which was not detected in XRD analysis of Fig. 1 due to the limited resolution. Fig. 7a illustrates the plan-view bright field TEM image for the coating annealed at 700 °C, representatively, together with the inserted corresponding selected area electron diffraction (SAED) pattern, in which the columns growth of coating was clearly identified. The SAED pattern confirmed the presence of the strongest V_2AlC (103) diffraction ring and weak V_2AlC (110), (100) and (109) preferred orientation. Moreover, we did not observe any diffuse rings characteristic of amorphous phases. Reasons for the amorphous carbon characteristics revealed by Raman (Fig. 2) may be too little to detect or only existed in the top surface layer. The grain size was about 10 nm from Fig. 7b at the annealing temperature of 700 °C. Moreover, it was found that the d value of lattice fringes was perfectly consistent with (101) plane of the V_2AlC MAX phase, as calculated from Fig. 7c.

In order to gather more insight into the dependence of mechanical properties and toughness of coating upon thermal annealing, the nano-indentor and Vickers indentation were taken for the pristine and annealed coatings. As shown in Fig. 8, the hardness and elastic modulus were 10.17 ± 0.72 GPa and 163.71 ± 18.84 GPa for the pristine coating. After annealing temperature in range of 600–800 °C, however, the hardness and elastic modulus first significantly increased and then followed by a monotonically decrease. The maximum value of the hardness and elastic modulus were found at annealing of 600 °C, which was 15.88 ± 0.61 GPa and 213.53 ± 19.9 GPa, respectively. Recalling the combined analysis of structure and chemical states, the hardness trend in Fig. 8 resulted from the structure growth: hardening due to the formed nanocrystalline composites in coatings after annealing and softening due to the emergence of layered V_2AlC MAX phases in coatings beyond of 600 °C. Noted that the hardness of 11.38 GPa for the pure V_2AlC MAX coating presented here was consistent with the obtained results by Sigumonrong et al. [6]. In addition, it is noted of particular that the obtained hardness are almost 5 times larger than the hardness of 2–4 GPa for the bulk V_2AlC phase materials [25]. These phenomena can be understood by the Hall–Petch's effect [26,27], where the strength of materials is inversely proportional to the square of crystalline size before a decreased threshold value. Different with the process of bulk MAX phases, the rapid cooling (quenching effect) during PVD vapor condensation [6] benefits the formed part of nanocrystallines

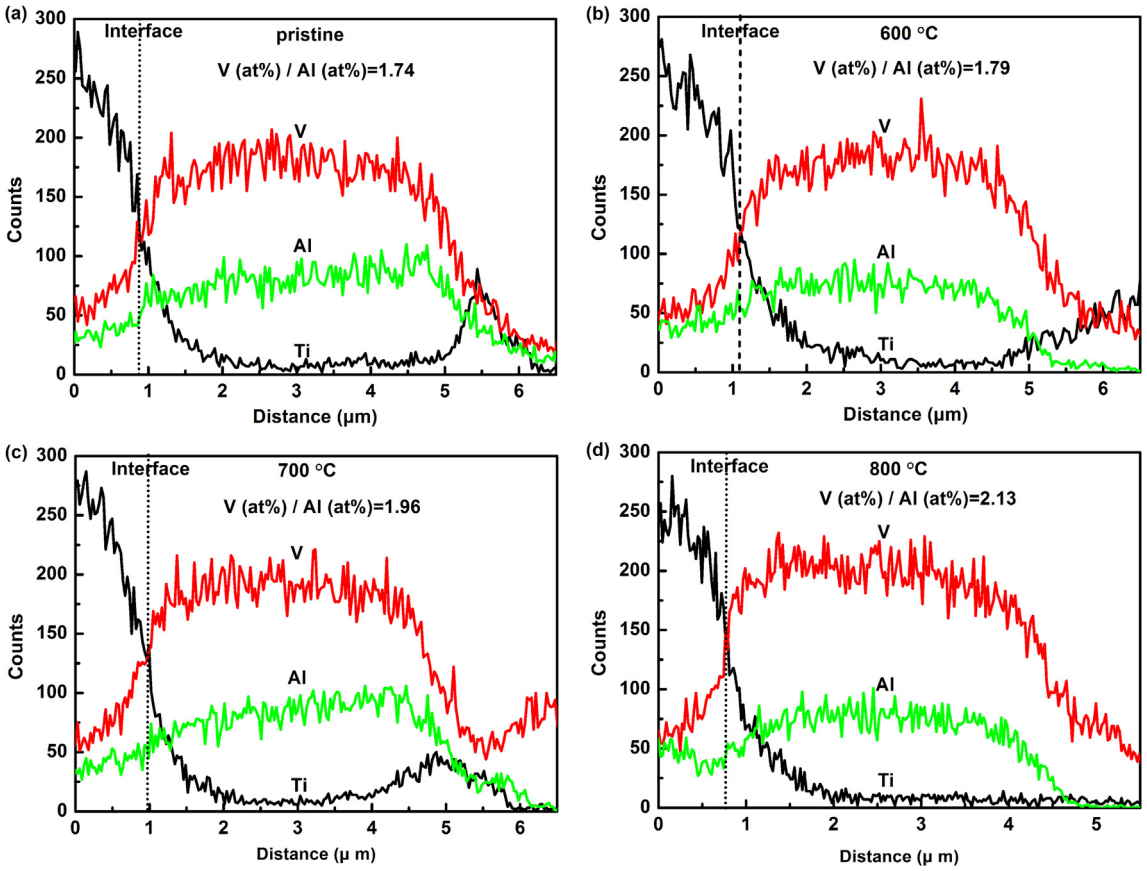

Fig. 5. Elemental analysis of cross sectional view of the pristine V–Al–C coatings (a) and annealed at (b) 600 °C, (c) 700 °C and (d) 800 °C by using EDX line scan.

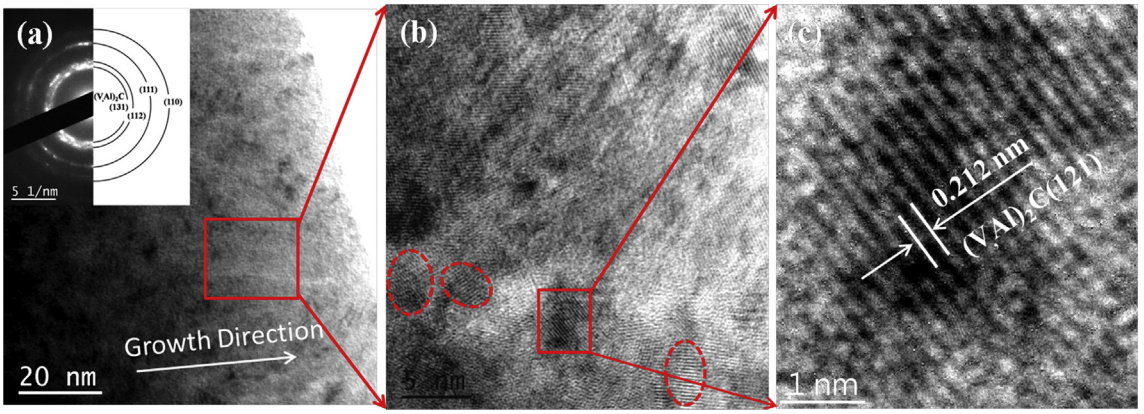

Fig. 6. TEM results of the pristine coating, (a) Bright-field image with the corresponding SAED pattern, (b) HRTEM image and (c) enlarged view.

distributed in the coating structure, which attributes to the good mechanical properties. Similar interpretation also holds for the hardness found in Cr_2AlC, Ti_3SiC_2 and Ti_3AlC_2 coatings, where a factor of 3–6 larger than the bulk value [28–30]. Further drop in hardness at annealed temperature of 800 °C must be attributed to the grain growth and content increase of layered MAX V_2AlC phase in coatings.

The inserted image in Fig. 8 shows the Vickers indentation morphology with a loaded 200 g force. For the pristine coating, some microcracks formed clearly along and inside the indentation area. The edge was not so distinct and presented as arc shape in profile, indicating a poor toughness [31]. After annealed at 600 °C, the V_2AlC MAX phase (26.2 wt%) appeared and the indentation-induced microcracks only occurred along the diagonal. All the edges transformed from arc shape into straight-line, which implied the occurrence of a larger plastic deformation. However, we noted that no cracks were observed around the indentation for the annealed coatings at 700 °C and 800 °C. Taking into account the structure evolution of increased pure V_2AlC MAX phase (> 98 wt% in this study) in coatings, it can thus be allowed that the layered MAX phase coating with good plasticity can endure more higher stress without brittle fracture. Besides, coating accumulation, similar to those of metallic materials, was generated along the edge due to the increased plastic deformation at annealed temperature

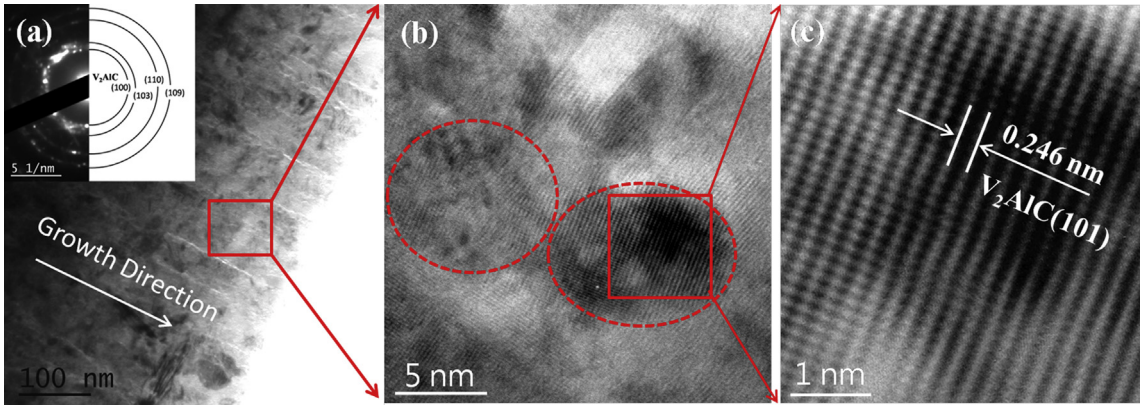

Fig. 7. TEM results of the annealed coating at 700 °C, (a) Bright-field image with the corresponding SAED pattern, (b) HRTEM image and (c) enlarged view.

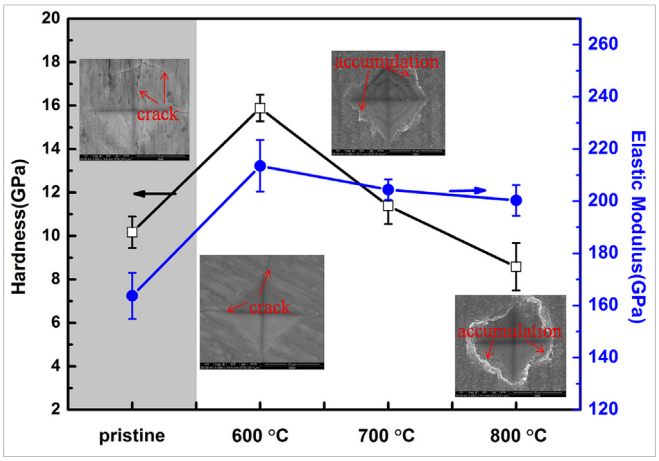

Fig. 8. Mechanical properties of the pristine and annealed V–Al–C coatings at 600 °C, 700 °C and 800 °C.

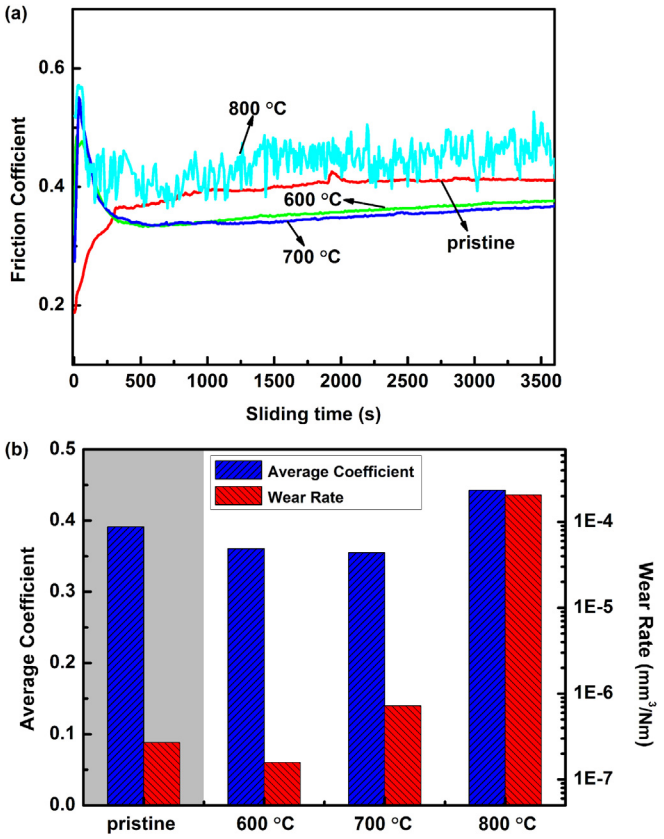

Fig. 9. (a) Friction behavior and (b) average friction coefficients and wear rates of the pristine and annealed V–Al–C coatings at 600 °C, 700 °C and 800 °C.

of 800 °C. Therefore, we could conclude that introducing the V_2AlC MAX phase will benefit the improved toughness of V–Al–C coating.

Fig. 9a shows the friction behavior curve of the pristine and annealed V–Al–C coatings at the temperature of 600 °C, 700 °C, and 800 °C versus the sliding time, the average coefficient of friction (μ) is shown in Fig. 9b. The friction coefficient gradually increased to the stable value ~0.39 after a long running-in period (about sliding 300 s) for the pristine V–Al–C coating. After annealing at 600 °C and 700 °C, nevertheless, the friction coefficients of coatings reached the steady state (0.36-0.35) after a short running stage. Since the running-in period is generally strong dependent upon the surface roughness of coating and adsorbed contaminants in surface, the difference of running-in period in the four samples could be interpreted from the coating structures. The Raman results proposed that the lowed friction coefficient for the annealed coatings might be attributed to the existence of the amorphous carbon phase, which mainly served as the lubricating layer between the sliding counterparts [32]. Further increasing the annealed temperature to 800 °C led to the fluctuation in the coefficient of friction beyond of 0.4 with a short running-in period. To further explore the wear resistance of pristine coating and annealed ones, Fig. 9b also illustrated the wear track behavior of coatings. The wear rates of the above three kinds of coatings were all of the same order of magnitude (10^{-7}mm^3/Nm). However, an increase of the annealed temperature to 800 °C resulted in an increase of the friction coefficient fluctuating severely during the sliding as well as an increase of the wear rates to 2.07×10^{-4} mm^3/Nm. The sever wear rates can be attributed to the disappearance of amorphous carbon and the decrease of the mechanical properties.

4. Conclusion

The V–Al–C coatings including $(V,Al)_2C$ nano-crystalline and amorphous phase were prepared by a traditional magnetron sputtering from a compound target with the composition of V_2AlC. The effects of annealing temperature on the evolution of structure, mechanical and tribological properties were investigated for the

coatings compared to the pristine coating. It was found that after the annealing at 600 °C, although a small amount of amorphous carbon phase appeared in the coatings, the emergence of the nanoscaled crystallines in V_2AlC MAX phase led to the improved mechanical and tribological behavior, where the maximum hardness at 15.88 ± 0.61 GPa and lower friction coefficient at 0.36 were achieved, respectively. Further increasing the annealed temperature to 700 °C, the purity of V_2AlC MAX phase was enhanced but the coating hardness decreased due to the significant increase in the content of amorphous carbon. Annealing at 800 °C promoted the further crystallinity of V_2AlC phase in the coating and the amorphous carbon almost disappeared. The important results presented here is that in range of 600–800 °C, thanks to the structure evolution process taking place, the highest hardness (15.88 ± 0.61 GPa), elastic modulus (213.53 ± 19.9 GPa) and the lowest wear rate (1.58E-7 mm^3/Nm) were obtained for case with annealing temperature of 600 °C. Furthermore, another promising result was that taking the traditional magnetron sputtering technique combined with the post annealing led to the controlled crystallinity of formed V_2AlC MAX phase, which made great contribution to the enhanced toughness combined with good mechanical and tribological behavior for the potential applications, such as the protective coatings for nuclear power plants, cutting tools etc.

Acknowledgments

This research was supported by the National Natural Science Foundation of China (51522106, 91226202), the National Science and Technology Major Project of China (2015ZX06004-001), and Ningbo Municipal Key Technologies R & D Program (2014B10032). We authors sincerely thank Prof. Magnus Odén at Linköping university for helpful discussion.

References

[1] M. Barsoum, Prog. Solid State Chem. 28 (2000) 201–281.
[2] M. Barsoum, T. El-Raghy, Metall. Mater. Trans. A 31 (2000) 1857–1865.
[3] P. Eklund, M. Beckers, U. Jansson, H. Högberg, L. Hultman, Thin Solid Films 518 (2010) 1851–1878.
[4] Y.X. Qiu, S. Zhang, J.W. Lee, B. Li, Y.X. Wang, D.L. Zhao, D. Sun, J. Alloy Compd. 618 (2015) 132–138.
[5] J.M. Schneider, R. Mertens, D. Music, J. Appl. Phys. 99 (2006) 013501–013504.
[6] D.P. Sigumonrong, J. Zhang, Y.C. Zhou, D. Music, J.M. Schneider, J. Phys. D. Appl. Phys. 42 (2009), 185408–8.
[7] Y. Jiang, R. Iskandar, M. Baben, T. Takahashi, J. Zhang, J. Emmerlich, J. Mayer, C. Polzer, P. Polcik, J.M. Schneider, J. Mater. Res. 27 (2012) 2511–2519.
[8] A. Abdulkadhim, M. Baben, V. Schnabel, M. Hans, N. Thieme, C. Polzer, P. Polcik, J.M. Schneider, Thin Solid Films 520 (2012) 1930–1933.
[9] R. Roger, E.W. Collings, G. Welsch, Materials Properties Handbook: Titanium Alloys, ASM International, Materials Park, 1993.
[10] A.L. Yerokhin, X. Nie, A. Leyland, A. Matthews, Surf. Coat. Technol. 130 (2000) 195–206.
[11] P. Guo, L.L. Sun, X.W. Li, S. Xu, P.L. Ke, A.Y. Wang, Thin Solid Films 584 (2015) 289–293.
[12] T.C. Santini, Int. J. Min. Process. 139 (2015) 1–10.
[13] W.C. Oliver, G.M. Pharr, J. Mater. Res. 7 (1992) 1564–1583.
[14] L. Shan, Y.X. Wang, J.L. Li, J.M. Chen, Surf. Coat. Technol. 242 (2014) 74–82.
[15] J.J. Li, Y.H. Qian, D. Niu, M.M. Zhang, Z.M. Liu, M.S. Li, Appl. Surf. Sci. 263 (2012) 457–464.
[16] M. Pandey, D. Bhatacharyya, D.S. Patil, K. Ramachandran, N. Venkatramani, A.K. Dua, J. Alloy Compd. 386 (2005) 296–302.
[17] J.J. Li, L.F. Hu, F.Z. Li, M.S. Li, Y.C. Zhou, Surf. Coat. Technol. 204 (2010) 3838–3845.
[18] Q.M. Wang, W. Garkas, A. Flores Renteria, C. Leyens, H.W. Lee, K.H. Kim, Corros. Sci. 53 (2011) 2948–2955.
[19] M. Daroonparvar, M.A.M. Yajid, N.M. Yusof, H.R. Bakhsheshi-Rad, E. Hamzah, H.A. Kamali, J. Alloy Compd. 615 (2014) 657–671.
[20] J. Frodelius, P. Eklund, M. Beckers, P.O.Å. Persson, H. Högberg, L. Hultman, Thin Solid Films 518 (2010) 1621–1626.
[21] P. Eklund, M. Beckers, J. Frodelius, H. Högberg, L. Hultman, J. Vac. Sci. Technol. A 25 (2007) 1381–1388.
[22] O. Wilhelmsson, P. Eklund, H. Högberg, L. Hultman, U. Jansson, Acta Mater. 56 (2008) 2563–2569.
[23] A. Abdulkadhim, M. to Baben, T. Takahashi, V. Schnabel, M. Hans, C. Polzer, P. Polcik, J.M. Schneider, Surf. Coat. Technol. 206 (2011) 599–603.
[24] R. Mertens, Z.M. Sun, D. Music, J.M. Schneider, Adv. Eng. Mater. 6 (2004) 903–907.
[25] C.F. Hu, L.F. He, M.Y. Liu, X.H. Wang, J.Y. Wang, M.S. Li, Y.W. Bao, Y.C. Zhou, J. Am. Ceram. Soc. 91 (2008) 4029–4035.
[26] E.O. Hall, Proc. Phys. Soc. Lond. B 64 (1951) 747–753.
[27] N.J. Petch, J. Iron Steel Inst. 174 (1953) 25–28.
[28] J.M. Schneider, D.P. Sigumonrong, D. Music, C. Walter, J. Emmerlich, R. Iskandar, J. Mayer, Scr. Mater. 57 (2007) 1137–1140.
[29] J. Emmerlich, H. Högberg, S. Sasvari, P.O.Å. Persson, L. Hultman, J.-P. Palmquist, U. Jansson, J.M. Molina-Aldareguia, Z. Czigány, J. Appl. Phys. 96 (2004) 4817–4826.
[30] O. Wilhelmsson, J.-P. Palmquist, T. Nyberg, U. Jansson, Appl. Phys. Lett. 85 (2004) 1066–1068.
[31] W.R. Feng, D.R. Yan, J.N. He, G.L. Zhang, G.L. Chen, W.C. Gu, S.Z. Yang, Appl. Surf. Sci. 243 (2005) 204–213.
[32] H.J. Choe, S.H. Kwon, J.J. Lee, Surf. Coat. Technol. 228 (2013) 282–285.